*Inorg. Chem.* **2004**, *43*, 1874–1884

Inorganic Chemistry
Article

# Octanuclear and Nonanuclear Supramolecular Copper(II) Complexes with Linear "Tritopic" Ligands: Structural and Magnetic Studies

**Victoria A. Milway, Virginie Niel, Tareque S. M. Abedin, Zhiqiang Xu, Laurence K. Thompson,* Hilde Grove, David O. Miller, and Stewart R. Parsons**

*Department of Chemistry, Memorial University of Newfoundland, St. John's, Newfoundland A1B 3X7, Canada*

Received March 27, 2003

The structures and magnetic properties of self-assembled copper(II) clusters and grids with the "tritopic" ligands 2poap (a), Cl2poap (b), m2poap (c), Cl2pomp (d), and 2pomp (e) are described [ligands derived by reaction of 4-R-2,6-pyridinedicarboxylic hydrazide (R = H, Cl, MeO) with 2-pyridinemethylimidate (a–c, respectively) or 2-acetylpyridine (d, R = Cl; e, R = H)]. Cl2poap and Cl2pomp self-assemble with $Cu(NO_3)_2$ to form octanuclear "pinwheel" cluster complexes $[Cu_8(Cl2poap\text{-}2H)_4(NO_3)_8]\cdot 20H_2O$ (**1**) and $[Cu_8(Cl2pomp\text{-}2H)_4(NO_3)_8]\cdot 15H_2O$ (**2**), built on a square [2 × 2] grid with four pendant copper arms, using "mild" reaction conditions. Similar reactions of Cl2pomp and 2pomp with $Cu(ClO_4)_2$ produce pinwheel clusters $[Cu_8(Cl2pomp\text{-}2H)_4(H_2O)_8](ClO_4)_8\cdot 7H_2O$ (**3**) and $[Cu_8(2pomp\text{-}2H)_4(H_2O)_8](ClO_4)_8$ (**4**), respectively. Heating a solution of **1** in MeOH/$H_2O$ produces a [3 × 3] nonanuclear square grid complex, $[Cu_9(Cl2poap\text{-}H)_3(Cl2poap\text{-}2H)_3](NO_3)_9\cdot 18H_2O$ (**5**), which is also produced by direct reaction of the ligand and metal salt under similar conditions. Reaction of m2poap with $Cu(NO_3)_2$ produces only the [3 × 3] grid $[Cu_9(m2poap\text{-}H)_2(m2poap\text{-}2H)_4](NO_3)_8\cdot 17H_2O$ (**6**) under similar conditions. Mixing the tritopic ligand 2poap with pyridine-2,6-dicarboxylic acid (picd) in the presence of $Cu(NO_3)_2$ produces a remarkable mixed ligand, nonanuclear grid complex $[Cu_9(2poap\text{-}H)_4(picd\text{-}H)_3(picd\text{-}2H)](NO_3)_9\cdot 9H_2O$ (**7**), in which aromatic $\pi$-stacking interactions are important in stabilizing the structure. Complexes **1**–**3** and **5**–**7** involve single oxygen atom (alkoxide) bridging connections between adjacent copper centers, while complex **4** has an unprecedented mixed $\mu$-(N–N) and $\mu$-O metal ion connectivity. Compound **1** ($C_{76}H_{92}N_{44}Cu_8O_{50}Cl_4$) crystallizes in the tetragonal system, space group $I\bar{4}$, with $a$ = 21.645(1) Å, $c$ = 12.950(1) Å, and $Z$ = 2. Compound **2** ($C_{84}H_{88}N_{36}O_{44}Cl_4Cu_8$) crystallizes in the tetragonal system, space group $I\bar{4}$, with $a$ = 21.2562(8) Å, $c$ = 12.7583(9) Å, and $Z$ = 2. Compound **4** ($C_{84}H_{120}N_{28}O_{66}Cl_8Cu_8$) crystallizes in the tetragonal system, space group $I4_1/a$, with $a$ = 20.7790(4) Å, $c$ = 32.561(1) Å, and $Z$ = 4. Compound **7** ($C_{104}H_{104}N_{46}O_{56}Cu_9$) crystallizes in the triclinic system, space group $P\bar{1}$, with $a$ = 15.473(1) Å, $b$ = 19.869(2) Å, $c$ = 23.083(2) Å, $\alpha$ = 88.890(2)°, $\beta$ = 81.511(2)°, $\gamma$ = 68.607(1)°, and $Z$ = 2. All complexes exhibit dominant intramolecular ferromagnetic exchange coupling, resulting from an orthogonal bridging arrangement within each polynuclear structure.

## Introduction

Polytopic ligands can be designed and synthesized with preprogrammed coordination information "stored" in the coordination pockets, such that when they react with a transition metal ion it interprets this information according to its own coordination algorithm. If the ligand pockets do not provide all the necessary donors, self-assembly can occur such that homoleptic coordination clusters form with the nuclearity being a function of the polytopic nature of the ligand and the preferred metal ion coordination number. This approach has had a significant measure of success with linear "polytopic" ligands based on pyridazine bridging subunits, which have produced molecular [2 × 2] $Cu^{I}_{4}$[1] ("ditopic" ligand) and [3 × 3] $Ag^{I}_{9}$[2] ("tritopic" ligand) grids, by a strict self-assembly process. The metal ions fit neatly into the

* To whom correspondence should be addressed. E-mail address: lthomp@mun.ca. Fax: 1-709-737-3702.

(1) Youinou, M.-T.; Rahmouni, N.; Fischer, J.; Osborn, J. A. *Angew. Chem., Int. Ed. Engl.* **1992**, *31*, 733.
(2) Baxter, P. N. W.; Lehn, J.-M.; Fischer, J.; Youinou, M.-T. *Angew. Chem., Int. Ed. Engl.* **1994**, *33*, 2284.



10.1021/ic030113u CCC: $27.50

Published on Web 02/27/2004

**Chart 1**

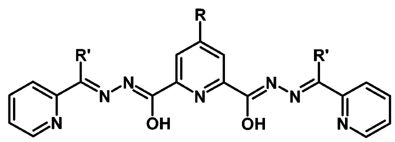

2poap (R=H, R'=$NH_2$), Cl2poap (R=Cl, R'=$NH_2$), m2poap (R=OMe, R'=$NH_2$), Cl2pomp (R=Cl, R'=$CH_3$), 2pomp (R=H, R=$CH_3$)

**Chart 2**

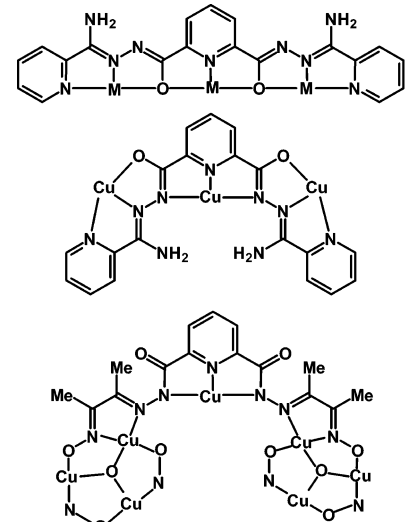

dpocco

tetrahedral pockets created by the assembly of pairs of ligands, which provide $N_2$ donor groupings above and below the planar arrangement of metal centers. Mixing similar ditopic and tritopic ligands can lead to a mixed [2 × 3] rectangular $Ag_6$ grid, along with small amounts of homoligand $Ag_4$ and $Ag_9$ grid complexes.[3] [2 × 2] homo- and heterometallic grids[4,5] of six-coordinate metal ions have been produced with ligands based on pyrimidine bridging subunits, where the donor groupings arise from the assembly of pairs of ligands that combine $N_3$ donor pockets. With Co(II) and Ni(II) salts magnetically coupled [2 × 2] grids form with such ligands, exhibiting intramolecular antiferromagnetic exchange,[6,7] despite long distances between metal centers (6.5 Å for Co). Evidence from NMR and ES mass spectrometry data has shown that with appropriate extension of these pyrimidine-based ligands [4 × 4] $Pb_{16}$ square grids can also be produced.[8]

Tritopic ligands (e.g. 2poap, Cl2poap; Chart 1), containing a linear arrangement of coordination pockets, self-assemble in high yield to form $M_9$ (M = Mn(II), Fe(III), Co(II), Ni(II), Cu(II)) grid structures, with a $[M_9(\mu\text{-O})_{12}]$ central core.[9−15] Each ligand binds to three metal ions with an alkoxide oxygen bridging between metal centers (Chart 2). The large M−O−M bridge angles lead to antiferromagnetic exchange interactions with Mn(II), Co(II), and Ni(II) complexes, but in the case of Cu(II) a preferred orthogonal magnetic bridging arrangement throughout the grid leads to dominant intramolecular ferromagnetic exchange in all cases. The high-yield syntheses of these homoleptic $M_9$ grids (usually >80%) indicates that the highly symmetric square arrangement, in which there is an exact match between the preferred coordination requirements of the metal ions and the available coordination pockets in the ligand, is highly favored thermodynamically.

Conditions for the formation of these $M_9$ grid systems usually involve heating in aqueous solvent mixtures. However in the case of copper(II) milder reaction conditions (e.g. room temperature), the use of solvent media with weaker donor character (e.g. $CH_3CN$, $CH_3CN/CH_3OH$ mixtures), and in some cases using anionic groups with significant donor capacity (e.g. acetate) can lead to the formation of linear trinuclear species,[16] in which the diazine nitrogen atoms act as bridges between adjacent metal centers (Chart 2). This dramatically different ligand conformation leads to very different magnetic behavior, dominated by antiferromagnetic exchange.[16] Extension of the basic hydrazide ligand to include terminal oxime groups leads to expansion of the coordination capacity of the ligand (e.g. dpocco, Chart 2) and the formation of a novel $Cu_{36}$ cluster, with diazine $N_2$ bridging, exhibiting antiferromagnetic exchange.[17]

In an unusual reaction in which 2poap was reacted with $Cu(NO_3)_2 \cdot 3H_2O$ in the presence of $Gd(NO_3)_3$ in $CH_3OH/CH_3CN$ a new oligomeric cluster/grid arrangement was obtained, in which four ligands self-assemble via half of each ligand to form a central square $[Cu_4(\mu\text{-O})_4]$ core, with four appended alkoxide-bridged Cu(II) centers in a "pinwheel" arrangement.[18] This system also behaves as an intramolecular ferromagnet. The Gd(III) ion was originally assumed to have a precoordination effect in the self-assembly process and contribute to the formation of the octanuclear complex. However it has now been shown that with different ligands, e.g. Cl2poap, Cl2pomp, and 2pomp (Chart 1), the presence of Gd(III) is not necessary and that $Cu_8$ clusters can be produced independently by suitable choice of solvent and

(3) Baxter, P. N. W.; Lehn, J.-M.; Kneisel, B. O.; Fenske, D. *Angew. Chem., Int. Ed. Engl.* **1997**, *36*, 1978.
(4) Hanan, G. S.; Volkmer, D.; Ulrich, S. S.; Lehn, J.-M.; Baum, G.; Fenske, D. *Angew. Chem., Int. Ed. Engl.* **1997**, *36*, 1842.
(5) Bassani, D. M.; Lehn, J.-M.; Fromm, K.; Fenske, D. *Angew. Chem., Int. Ed.* **1998**, *37*, 2364.
(6) Waldmann, O.; Hassmann, J.; Müller, P.; Hanan, G. S.; Volkmer, D.; Schubert, U. S.; Lehn, J.-M. *Phys. Rev. Lett.* **1997**, *78*, 3390.
(7) Waldmann, O.; Hassmann, J.; Müller, P.; Hanan, G. S.; Volkmer, D.; Schubert, U. S.; Lehn, J.-M. *Phys. Rev. B* **1998**, *58*, 3277.
(8) Garcia, A. M.; Romero-Salguero, F. J.; Bassani, D. M.; Lehn, J.-M.; Baum, G.; Fenske, D. *Chem. Eur. J.* **1999**, *5*, 1803.
(9) Zhao, L.; Matthews, C. J.; Thompson, L. K.; Heath, S. L. *J. Chem. Soc., Chem. Commun.* **2000**, 265.
(10) Zhao, L.; Xu, Z.; Thompson, L. K.; Heath, S. L.; Miller, D. O.; Ohba, M. *Angew. Chem., Int. Ed.* **2000**, *39*, 3114.
(11) Waldmann, O.; Koch, R.; Schromm, S.; Müller, P.; Zhao, L.; Thompson, L. K. *Chem. Phys. Lett.* **2000**, *332*, 73.
(12) Waldmann, O.; Zhao, L.; Thompson, L. K. *Phys. Rev. Lett.* **2002**, *88*, 066401−1−4.
(13) Zhao, L.; Xu, Z,; Thompson, L. K.; Miller, D. O. *Polyhedron* **2001**, *20*, 1359.
(14) Xu, Z.; Thompson, L. K.; Miller, D. O. *Polyhedron* **2002**, *21*, 1715.
(15) Thompson, L. K.; Zhao, L.; Xu, Z.; Miller, D. O.; Reiff, W. M. *Inorg. Chem.* **2003**, *42*, 128.
(16) Zhao, L.; Thompson, L. K.; Xu, Z.; Miller, D. O.; Stirling, D. R. *J. Chem. Soc., Dalton Trans.* **2001**, 1706.
(17) Abedin, T. S. M.; Thompson, L. K.; Miller, D. O.; Krupicka, E. *J. Chem. Soc., Chem. Commun.* **2003**, 708.
(18) Xu, Z.; Thompson, L. K.; Miller, D. O. *J. Chem. Soc., Chem. Commun.* **2001**, 1170.

temperature. Also in one case the $Cu_8$ pinwheel cluster complex can be converted to the more thermodynamically favored $Cu_9$ grid simply by heating in a polar solvent.

The structural and magnetic properties for $[Cu_8(Cl2poap\text{-}2H)_4(NO_3)_8]\cdot 20H_2O$ (**1**), $[Cu_8(Cl2pomp\text{-}2H)_4(NO_3)_8]\cdot 15H_2O$ (**2**), $[Cu_8(2pomp\text{-}2H)_4(H_2O)_8](ClO_4)_8$ (**4**), $[Cu_9(Cl2poap\text{-}H)_3(Cl2poap\text{-}2H)_3](NO_3)_9\cdot 18H_2O$ (**5**), and $[Cu_9(m2poap\text{-}H)_2(m2poap\text{-}2H)_4](NO_3)_8\cdot 17H_2O$ (**6**) are now reported, in addition to a novel complex with a mixture of ligands, $[Cu_9(2poap\text{-}H)_4(picd\text{-}H)_3(picd\text{-}2H)](NO_3)_9\cdot 9H_2O$ (**7**), which highlights the importance of ligand−ligand interactions and ligand "bite" in the construction of the grid.

## Experimental Section

**Physical Measurements.** Infrared spectra were recorded as Nujol mulls using a Mattson Polaris FT-IR instrument, and UV/vis spectra were obtained as Nujol mulls using a Cary 5E spectrometer. Microanalyses were carried out by Canadian Microanalytical Service, Delta, Canada. Variable-temperature magnetic data (2−300 K) were obtained using a Quantum Design MPMS5S SQUID magnetometer using field strengths in the range 0.1−5 T. Background corrections for the sample holder assembly and diamagnetic components of the complexes were applied.

**Synthesis of Complexes. $[Cu_8(Cl2poap\text{-}2H)_4(NO_3)_8]\cdot 20H_2O$ (1).** Cl2poap was synthesized by adopting a published method starting from 4-chloro-2,6-pyridinedicarboxylic acid.[9,10] Cl2poap (0.44 g, 1.0 mmol) was suspended in a solution of $Cu(NO_3)_2\cdot 3H_2O$ (0.87 g, 3.0 mmol) in a mixture of 10 mL of acetonitrile and 10 mL of methanol at room temperature. The resulting mixture was stirred for a few minutes at room temperature, forming a clear deep green solution. Green crystals, suitable for a structural determination, formed from the filtrate after standing overnight at room temperature (yield 83.5%). IR (Nujol mull, $cm^{-1}$): 3400, 3192 (br, w) ($\nu(H_2O)$ and $\nu(NH_2)$); 1771 (w), 1749 (w), 1733 (w) ($\nu(NO_3)$). 1666 ($\nu$(C═O)); 1028, 1020 (m) ($\nu$(py)). Anal. Found: C, 29.20; H, 2.94; N, 20.00. Calcd for $(C_{19}H_{14}N_9O_2Cl)_4Cu_8(NO_3)_8(H_2O)_{20}$: C, 29.42; H, 3.10; N, 19.87.

**$[Cu_8(Cl2pomp\text{-}2H)_4(NO_3)_8]\cdot 15H_2O$ (2) and $[Cu_8(Cl2pomp\text{-}2H)_4(H_2O)_8](ClO_4)_8\cdot 7H_2O$ (3).** Cl2pomp was synthesized by reaction of 2-acetylpyridine with 4-chloropyridine-2,6-dicarboxylic hydrazide by standard procedures (yield 93%, mp >300 °C). Anal. Found: C, 57.53; H, 4.07; N, 22.27. Calcd for $C_{21}H_{18}N_7O_2Cl$: C, 57.91; H, 4.17; N, 22.52.[9,10,16] $Cu(NO_3)_2\cdot 3H_2O$ (0.21 g, 0.87 mmol) was dissolved in methanol (10 mL). Cl2pomp (0.10 g, 0.23 mmol) was added and dissolved rapidly on warming. A powdery green precipitate formed, which was redissolved by addition of water (10 mL) and warming. Green rectangular prismatic crystals, suitable for structural analysis, formed after 3 days (yield 83%). IR (Nujol mull, $cm^{-1}$): 3403 ($\nu(NH_2)$ and $\nu(H_2O)$); 1627 ($\nu$(C═O)), 1601 ($\nu$(C═N)); 1025 (w) ($\nu$(py)). Anal. Found: C, 33.55; H, 2.87; N, 16.72. Calcd for $(C_{21}H_{16}N_7O_2Cl)_4Cu_8(NO_3)_8(H_2O)_{15}$ (**2**): C, 33.58; H, 3.16; N, 16.79. **3** was prepared in the same manner with $Cu(ClO_4)_2\cdot 6H_2O$ and obtained as green crystals (yield 80%). Anal. Found: C, 30.40; H, 2.63; N, 12.09. Calcd for $(C_{21}H_{16}N_7O_2Cl)_4Cu_8(ClO_4)_8(H_2O)_{15}$: C, 30.57; H, 2.87; N, 11.89.

**$[Cu_8(2pomp\text{-}2H)_4(H_2O)_8](ClO_4)_8$ (4).** 2pomp was synthesized by standard procedures by reaction of 2-acetylpyridine with pyridine-2,6-dicarboxylic hydrazide.[9,10,16] 2pomp (0.24 g, 0.50 mmol) was added to a solution of $Cu(ClO_4)_2\cdot 6H_2O$ dissolved in methanol/water mixture (10 mL/5 mL) with stirring. A clear deep blue green solution formed, which was filtered after several hours and allowed to stand at room temperature. Dark green crystals suitable for structural determination were obtained after 2 weeks (yield 70%). IR (Nujol mull, $cm^{-1}$): 3600, 3450 ($\nu(H_2O)$), 1620 ($\nu$(C═O)), 1602, 1571 ($\nu$(C═N)), 1077 ($\nu(ClO_4)$). UV/vis ($\lambda_{max}$ (nm); water): 683. Anal. Found: C, 33.23; H, 2.70; N, 13.03. Calcd for $(C_{21}H_{16}N_7O_2)_4Cu_8(ClO_4)_8(H_2O)_8$: C, 33.11; H, 3.02; N, 12.88.

**$[Cu_9(Cl2poap\text{-}H)_3(Cl2poap\text{-}2H)_3](NO_3)_9\cdot 20H_2O$ (5).** The reaction between Cl2poap and $Cu(NO_3)_2\cdot 3H_2O$ was repeated using a different solvent mixture (10 mL of methanol and 10 mL of deionized water) with warming. An orange-red crystalline product formed, suitable for a structural analysis (yield 86%). IR (Nujol mull, $cm^{-1}$): 3337 (w) ($\nu(NH_2)$ and $\nu(H_2O)$); 1670 ($\nu$(C═O)); 1015 (w) ($\nu$(py)). Anal. Found: C, 33.57; H, 2.98; N, 21.31. Calcd for $(C_{19}H_{14}N_9O_2Cl)_3(C_{19}H_{15}N_9O_2Cl)_3Cu_9(NO_3)_9(H_2O)_{20}$: C, 33.33; H, 3.12; N, 21.48.

**$[Cu_9(m2poap\text{-}H)_2(m2poap\text{-}2H)_4](NO_3)_8\cdot 17H_2O$ (6).** m2poap[14] (0.100 g, 0.231 mmol) was dissolved in methanol (10 mL) and added to a solution of $Cu(NO_3)_2\cdot 3H_2O$ (0.170 g, 0.693 mmol) in deionized water (10 mL). The resulting green solution was warmed, refluxed for 15 min, and left to evaporate slowly at room temperature. Brown crystals suitable for structural analysis were obtained after 2 weeks (yield 30%). IR (Nujol mull, $cm^{-1}$): 3337 (w) ($\nu(NH_2)$ and $\nu(H_2O)$); 1667 ($\nu$(C═O)); 1587 ($\nu$(C═N)); 1012 ($\nu$(py)). UV/vis ($\lambda_{max}$ (nm); Nujol mull): 395, 480 (sh), 743. Anal. Found: C, 36.09; H, 3.07; N, 22.00. Calcd for $(C_{20}H_{18}N_9O_3)_2(C_{20}H_{17}N_9O_3)_4Cu_9(NO_3)_8(H_2O)_{17}$: C, 36.33; H, 3.56; N, 21.89.

**$[Cu_9(2poap\text{-}H)_4(picd\text{-}H)_3(picd\text{-}2H)](NO_3)_9\cdot 9H_2O$ (7).** $Cu(NO_3)_2\cdot 3H_2O$ (0.90 g, 3.7 mmol) was dissolved in $MeOH/H_2O$ (10 mL/5 mL). 2poap (0.40 g, 1.0 mmol) and pyridine-2,6-dicarboxylic acid (0.17 g, 1.0 mmol) were well mixed and added together to the metal ion solution with stirring. A clear green solution was formed on heating, which deposited dark green crystals, suitable for structural analysis, after several days (yield 75%). IR (Nujol mull, $cm^{-1}$): 3337 (w) ($\nu(NH_2)$ and $\nu(H_2O)$); 1670 ($\nu$(C═O)); 1015 (w) ($\nu$(py)). Anal. Found: C, 34.93; H, 2.80; N, 19.56. Calcd for $(C_{19}H_{16}N_9O_2)_4(C_7H_4NO_4)_3(C_7H_3NO_4)Cu_9(NO_3)_9(H_2O)_9$: C, 35.07; H, 2.75; N, 19.25.

**Crystallographic Data and Refinement of the Structures.** The diffraction intensities of a green prismatic crystal of **1** of dimensions 0.33 × 0.26 × 0.22 mm were collected with graphite-monochromatized Mo Kα X-radiation (rotating anode generator) using a Bruker P4/CCD diffractometer at 193(1) K to a maximum 2$\theta$ value of 52.8°. The data were corrected for Lorentz and polarization effects. The structure was solved by direct methods.[19,20] All atoms except hydrogens were refined anisotropically. Hydrogen atoms were placed in calculated positions with isotropic thermal parameters set to 20% greater than their bonded partners and were not refined. Neutral atom scattering factors[21] and anomalous-dispersion terms[22,23] were taken from the usual sources. All other calculations were performed with the teXsan[24] crystallographic software package using a PC computer. The maximum and minimum peaks on the

(19) (a) SHELX97: Sheldrick, G. M., 1997. (b) SIR97: Altomare, A.; Cascarano, M.; Giacovazzo, C.; Guagliardi, A. *J. Appl. Crystallogr.* **1993**, *26*, 343.
(20) DIRDIF94: Beurskens, P. T.; Admiraal, G.; Beurskens, G.; Bosman, W. P.; de Gelder, R.; Israel, R.; Smits, J. M. M. *The DIRDIF-94 program system*; Technical Report of the Crystallography Laboratory, University of Nijmegen: Nijmegen, The Netherlands, 1994.
(21) Cromer, D. T.; Waber, J. T. *International Tables for X-ray Crystallography*; The Kynoch Press: Birmingham, England, 1974; Vol. IV, Table 2.2A.
(22) Ibers, J. A.; Hamilton, W. C. *Acta Crystallogr.* **1964**, *17*, 781.
(23) Creagh, D. C.; McAuley, W. J. *International Tables for Crystallography*; Wilson, A. J. C., Ed.; Kluwer Academic Publishers: Boston, MA, 1992; Vol. C, Table 4.2.6.8, pp 219−222.

**Table 1.** Summary of Crystallographic Data for **1**, **2**, **4**, and **7**

| param | **1** | **2** | **4** | **7** |
|---|---|---|---|---|
| empirical formula | $C_{76}H_{92}N_{44}Cu_8O_{50}Cl_4$ | $C_{84}H_{88}N_{36}O_{44}Cl_4Cu_8$ | $C_{84}H_{120}N_{28}O_{66}Cl_8Cu_8$ | $C_{104}H_{104}N_{46}O_{56}Cu_9$ |
| $M_r$ | 3072.01 | 2956.01 | 3370.01 | 3466.15 |
| cryst system | tetragonal | tetragonal | tetragonal | triclinic |
| space group | $I\bar{4}$ | $I\bar{4}$ | $I4_1/a$ | $P\bar{1}$ |
| $a$/Å | 21.645(1) | 21.2562(8) | 20.7790(4) | 15.473(1) |
| $b$/Å | 21.645(1) | 21.2562(8) | 20.7790(4) | 19.869(2) |
| $c$/Å | 12.950(1) | 12.7583(4) | 32.561(1) | 23.083(2) |
| $\alpha$/deg | 90 | 90 | 90 | 88.890(2) |
| $\beta$/deg | 90 | 90 | 90 | 81.511(2) |
| $\gamma$/deg | 90 | 90 | 90 | 68.607(1) |
| $V$/Å$^3$ | 6067.0(6) | 5764.5(4) | 14058.8(6) | 6530.7(8) |
| $\rho_{calcd}$/g cm$^{-3}$ | 1.681 | 1.703 | 1.592 | 1.763 |
| $T$/K | 193(1) | 193(1) | 193(1) | 193(1) |
| Z | 2 | 2 | 4 | 2 |
| $\mu$/cm$^{-1}$ | 15.68 | 16.41 | 14.39 | 15.50 |
| reflcns collcd: tot., unique, $R_{int}$ | 20 830, 6234, 0.040 | 17 468, 58 73, 0.064 | 34 336, 7189, 0.025 | 37 176, 26 239, 0.044 |
| reflcns obsd ($I > 2.00\sigma(I)$) | 5606 | 4743 | 7189 | 15 585 |
| final $R_1$,[a] $wR_2$[b] | 0.043, 0.127 | 0.055, 0.148 | 0.061, 0.203 | 0.075, 0.211 |

[a] $R_1 = \sum||F_o| - |F_c||/\sum|F_o|$. [b] $wR_2 = [\sum[w(|F_o|^2 - |F_c|^2)^2]/\sum[w(|F_o|^2)^2]]^{1/2}$.

final difference Fourier map corresponded to 1.38 and −0.36 e$^-$/Å$^3$, respectively. Abbreviated crystal data for **1** are given in Table 1.

Diffraction data were collected for **2** (green prism; 0.29 × 0.09 × 0.08 mm), **4** (dark prism; 0.53 × 0.45 × 0.40 mm), **5** (red brown prism; 0.18 × 0.15 × 0.07 mm), **6** (brown prism; 0.74 × 0.34 × 0.33 mm), and **7** (yellow-brown prism; 0.40 × 0.20 × 0.15 mm) in a similar manner. A very weak data set for **5** (10% observed with an $R_{int}$ = 49%) led to poor refinement values and a rather low parameter/data ratio (<5:1) (space group *Pbca*, $a$ = 24.78 Å, $b$ = 26.75 Å, $c$ = 46.76 Å). The main grid fragment is however clearly defined in the current structural solution. Therefore, only preliminary structural details for **5** are discussed and refinement details are not reported. Significant disorder problems were encountered in the refinement of **6**, both in the methoxy groups and nitrates, but the expected grid cation shows up clearly, and so at this stage only a preliminary report of this structure is included (space group $P\bar{1}$, $a$ = 19.083(2) Å, $b$ = 19.141(2) Å, $c$ = 23.491(2) Å, $\alpha$ = 76.602(2)°, $\beta$ = 89.710(2)°, $\gamma$ = 89.960(2)°, $R_1$ = 0.098, $wR_2$ = 0.346). Abbreviated full structural data for **2**, **4**, and **7** are reported in Table 1.

For **2** all non-hydrogen atoms were refined anisotropically, and hydrogen atoms on aromatic carbons and methyl groups were placed in calculated positions (thermal parameters set 20% greater than their bonding partners) and not refined. Hydrogen atoms on water molecules were found and fixed but not refined. For **4** refinement proceeded normally, and hydrogen atoms were introduced in calculated positions with isotropic thermal parameters set to 20% greater than those of their bonding partners at the time of their inclusion. They were not refined. For **7** hydrogen atoms were introduced in calculated or difference map positions, with isotropic thermal parameters set 20% greater than those of their bonded partners at the time of their inclusion. They were not refined. There are a total of 12 hydrogen atoms missing from the model, 4 from the carboxylates and 8 from lattice water molecules.

## Results and Discussion

**Structural Results. $[Cu_8(Cl2poap\text{-}2H)_4(NO_3)_8]\cdot 20H_2O$ (1).** The structural representation of **1** is shown in Figure 1, and selected bond distances and angles are listed in Table 2. The octanuclear cluster consists of a central square $[Cu_4(\mu\text{-}O)_4]$ core with six-coordinate copper(II) centers attached to the ends of four deprotonated ligands, very similar to tetranuclear structures reported previously with poap and related ligands,[25,26] and four additional square-pyramidal copper(II) centers bonded to the other ends of the ligands, resulting in a pinwheel-like structural arrangement. All adjacent copper centers are connected by alkoxide bridges,

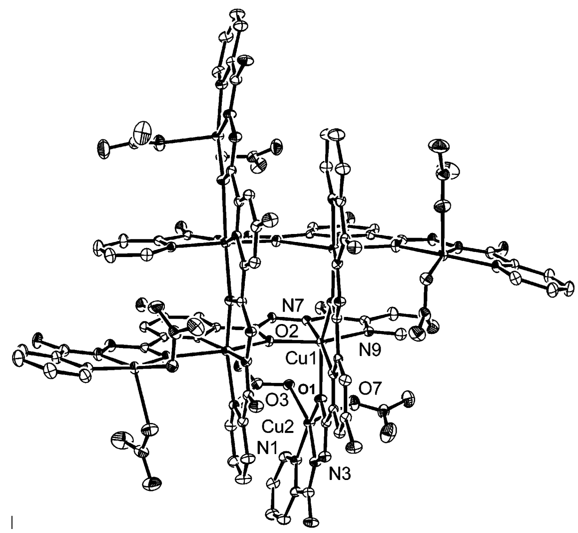


**Figure 1.** Structural representation of the $Cu_8$ cation in **1** (40% probability thermal ellipsoids).

**Table 2.** Selected Bond Distances (Å) and Angles (deg) for **1**

| | | | |
|---|---|---|---|
| Cu(1)−N(7) | 1.912(4) | Cu(2)−O(3) | 2.000(4) |
| Cu(1)−O(2) | 2.003(3) | Cu(2)−N(1) | 2.020(4) |
| Cu(1)−N(5) | 2.017(4) | Cu(2)−O(7) | 2.308(4) |
| Cu(1)−N(9) | 2.045(4) | N(3)−N(4) | 1.403(6) |
| Cu(1)−O(2) | 2.284(3) | N(6)−N(7) | 1.397(5) |
| Cu(1)−O(1) | 2.337(3) | Cu(1)−Cu(1)′ | 4.011(4) |
| Cu(2)−N(3) | 1.903(4) | Cu(2)−Cu(1) | 4.056(4) |
| Cu(2)−O(1) | 1.978(3) | | |
| Cu(1)−O(1)−Cu(2) | 139.98(17) | Cu(1)−O(2)−Cu(1)′ | 138.67(16) |

(24) teXsan for Windows: *Crystal Structure Analysis Package*; Molecular Structure Corp.: The Woodlands, TX, 1997.

(25) Matthews, C. J.; Avery, K.; Xu, Z.; Thompson, L. K.; Zhao, L.; Miller, D. O.; Biradha, K.; Poirier, K.; Zaworotko, M. J.; Wilson, C.; Goeta, A. E.; Howard, J. A. K. *Inorg. Chem.* **1999**, *38*, 5266.

(26) Thompson, L. K.; Matthews, C. J.; Zhao, L.; Xu, Z.; Miller, D. O.; Wilson, C.; Leech, M. A.; Howard, J. A. K.; Heath, S. L.; Whittaker, A. G.; Winpenny, R. E. P. *J. Solid State Chem.* **2001**, *159*, 308.

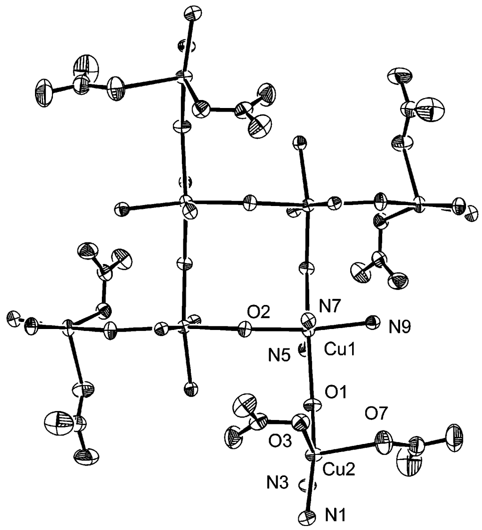


**Figure 2.** Core structure of **1** showing externally bound nitrates (40% probability thermal ellipsoids).

with large Cu−O−Cu bridge angles (Cu(1)−O(1)−Cu(2) 139.98(17)°, Cu(1)−O(2)−Cu(1)′ 138.67(16)°) but in a strictly orthogonal bridging arrangement (vide infra). C−O distances in the core are 1.298(5) Å, and 1.309(5) Å in the pinwheel arms, indicating significant single bond character. The peripheral copper atoms are bound to the external ligand pockets by three donor atoms only ($N_2O$), and the other coordination sites are occupied by eight monodentate nitrate ligands. Figure 2 illustrates the core structure more clearly.

Adjacent Cu−Cu separations within the square core are 4.011(4) Å, while distances from the core copper atoms to the outer copper atoms are 4.056(4) Å. The six-coordinate Cu(1) centers have tetragonal stereochemistry, with elongation along the O(1)−Cu(1)−O(2)′ axis. This leads to Cu(1)−O(2) distances within the square core which alternate as 2.284(3) and 2.003(3) Å, clearly defining the orthogonal linkages. The long Cu(1)−O(1) contact (2.337(3) Å) creates an orthogonal linkage to the external copper ions as well.

**[$Cu_8$(Cl2pomp-2H)$_4$($NO_3$)$_8$]·15$H_2O$ (2).** The structure of the octanuclear cation in **2** is very similar to that in **1**, with two monodentate nitrate groups bound to the peripheral copper ions. The core structure is represented in POVRAY format in Figure 3. Important bond lengths and angles are listed in Table 3. Dimensions in the cluster are almost identical to those in **1**, which is perhaps not surprising given the slight difference in the ligands, with differing R′ groups ($NH_2$ and $CH_3$) on the ligand backbone. Cu−O−Cu angles fall in the range 139.1−139.4°, and C−O distances in the core (1.288(8) Å) and in the pinwheel arms (1.290(8) Å) indicate significant single-bond character. The analogous perchlorate complex [$Cu_8$(Cl2pomp-2H)$_4$($H_2O$)$_8$]($ClO_4$)$_8$·7$H_2O$ **(3)** appears to have the same octanuclear structure, and since infrared evidence indicates that the perchlorate groups are ionic, it is realistic to assume that each of the external copper ions has two coordinated water molecules.

**[$Cu_8$(2pomp-2H)$_4$($H_2O$)$_8$] ($ClO_4$)$_8$ (4).** The stucture of the octanuclear cation in **4** is shown in Figure 4, and it is immediately obvious that it is different from **1** and **2** although it still has a pinwheel arrangement. Two water molecules

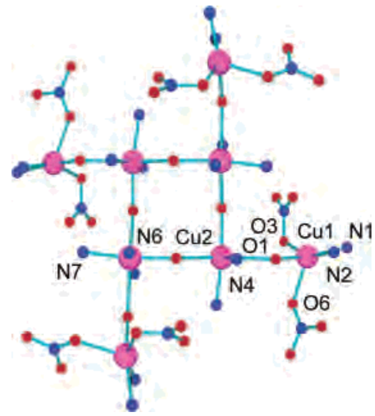


**Figure 3.** Core structure of **2** (POVRAY) showing externally bound nitrates (magenta = Cu, blue = N, red = O).

**Table 3.** Selected Bond Distances (Å) and Angles (deg) for **2**

| | | | |
|---|---|---|---|
| Cu(1)−N(2) | 1.941(6) | Cu(2)−N(7) | 2.015(5) |
| Cu(1)−O(1) | 2.003(5) | Cu(2)−N(4) | 2.036(5) |
| Cu(1)−N(1) | 2.008(6) | Cu(2)−O(2) | 2.289(4) |
| Cu(1)−O(3) | 2.021(5) | Cu(2)−O(1) | 2.340(4) |
| Cu(1)−O(6) | 2.213(5) | Cu(1)−Cu(2) | 4.075(3) |
| Cu(2)−N(6) | 1.933(5) | Cu(2)−Cu(2)′ | 4.014(3) |
| Cu(2)−O(2) | 1.993(4) | | |
| Cu(1)−O(1)−Cu(2) | 139.4(2) | Cu(2)−O(2)−Cu(2)′ | 139.1(2) |

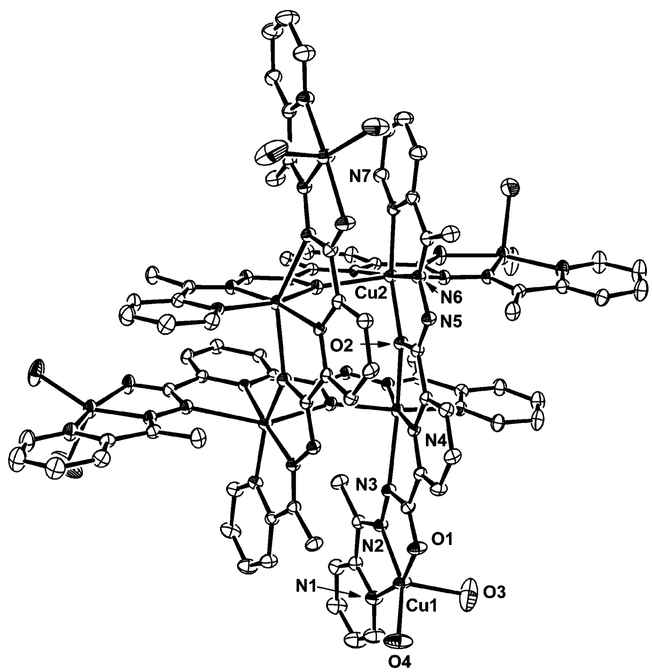


**Figure 4.** Structural representation of the cation in **4** (40% probability thermal ellipsoids).

are bound to each of the peripheral copper(II) ions, instead of nitrates, and the perchlorate ions are uncoordinated. However the internal ligand connectivity is different from the norm (**1**, **2**) and involves a central [$Cu_4$-($\mu$-O)$_4$] core of six coordinate metal ions, but the connections to the peripheral square-pyramidal copper ions involve N−N bridges, observed for the first time in this class of compounds. C−O distances are slightly shorter in **4** (1.289(6) Å in the core and 1.270(6) Å in the pinwheel arms) indicating more double CO bond character. However in this case, as in **1** and **2**, there is significant charge delocalization within

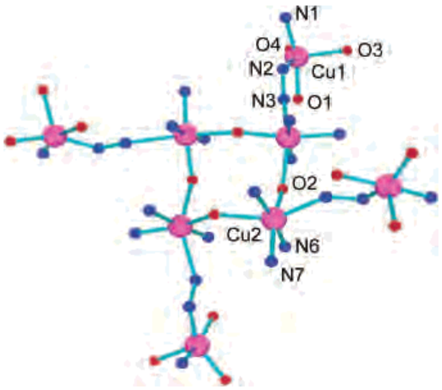


**Figure 5.** Core structure in **4** (POVRAY; magenta = Cu, blue = N, red = O).

**Table 4.** Selected Bond Distances (Å) and Angles (deg) for **4**

| | | | |
|---|---|---|---|
| Cu(1)−N(2) | 1.927(4) | Cu(2)−N(4) | 2.001(3) |
| Cu(1)−O(1) | 1.971(3) | Cu(2)−O(2) | 2.034(3) |
| Cu(1)−O(4) | 1.985(4) | Cu(2)−N(7) | 2.045(4) |
| Cu(1)−N(1) | 2.004(4) | Cu(2)−O(2) | 2.347(3) |
| Cu(1)−O(3) | 2.135(5) | Cu(2)−N(3) | 2.443(4) |
| Cu(2)−N(6) | 1.928(3) | | |
| N(2)−Cu(1)−O(1) | 79.75(14) | N(6)−Cu(2)−N(7) | 79.76(15) |
| N(2)−Cu(1)−O(4) | 153.9(2) | N(4)−Cu(2)−N(7) | 96.05(14) |
| O(1)−Cu(1)−O(4) | 94.76(16) | O(2)−Cu(2)−N(7) | 158.54(13) |
| N(2)−Cu(1)−N(1) | 81.08(16) | N(6)−Cu(2)−O(2) | 96.81(13) |
| O(1)−Cu(1)−N(1) | 159.86(16) | N(4)−Cu(2)−O(2) | 75.83(12) |
| O(4)−Cu(1)−N(1) | 99.78(17) | O(2)−Cu(2)−O(2) | 87.88(16) |
| N(2)−Cu(1)−O(3) | 114.2(3) | N(7)−Cu(2)−O(2) | 96.89(13) |
| O(1)−Cu(1)−O(3) | 95.81(19) | N(6)−Cu(2)−N(3) | 113.67(14) |
| O(4)−Cu(1)−O(3) | 91.6(3) | N(4)−Cu(2)−N(3) | 74.47(13) |
| N(1)−Cu(1)−O(3) | 97.6(2) | O(2)−Cu(2)−N(3) | 89.06(12) |
| N(6)−Cu(2)−N(4) | 171.14(15) | N(7)−Cu(2)−N(3) | 97.44(14) |
| N(6)−Cu(2)−O(2) | 78.90(13) | O(2)−Cu(2)−N(3) | 148.13(11) |
| N(4)−Cu(2)−O(2) | 105.41(13) | Cu(2)−O(2)−Cu(2) | 142.17(14) |

the ligand hydrazone fragment. The core structure is shown in Figure 5, revealing the different bridging connections. Important bond distances and angles are listed in Table 4. Cu−Cu distances within the square core (4.146(2) Å) are much shorter than those from the core to the peripheral copper ions (5.230(2) Å) as expected, and Cu−O−Cu angles are quite large (142.17(14)°).

Copper−oxygen bond connections within the square [$Cu_4$-($\mu$-O)$_4$] core alternate long−short (2.034(3), 2.347(3) Å), as before, with orthogonal connections between all the six-coordinate metal ions in the core. Distances from Cu(2) to N(3) (2.443(4) Å) indicate an axial contact from each corner copper ion to the diazine bridge, leading to strict "d" orbital orthogonality between the core and peripheral copper centers. Torsional angles to the peripheral copper ions via the N−N single bond bridges are large (154.6°), but the axial−equatorial connections cannot lead to any significant antiferromagnetic interaction through this bridge (vide infra). There are no lattice contacts of any significance that could lead to possible intermolecular associations that might influence the magnetic properties.

**[Cu$_9$(Cl2poap-H)$_3$(Cl2poap-2H)$_3$](NO$_3$)$_9$·18H$_2$O (5).** The structural details of **5** cannot be reported in full because of poor X-ray diffraction data quality, associated in part with crystal instability. However, the nonanuclear cation structure is clearly revealed. Nine copper(II) centers are held within the normal grid structure by six ligands arranged in two groups of three above and below the roughly planar [$Cu_9$-($\mu$-O)$_{12}$] core, with a tetragonally compressed ($d_{z^2}$) central copper ion. This is the typical structural arrangement for systems of this type, with overall dimensions that are very similar to other $Cu_9$ grids with related ligands and nominally orthogonal bridge connections between all adjacent metal centers.[9−15]

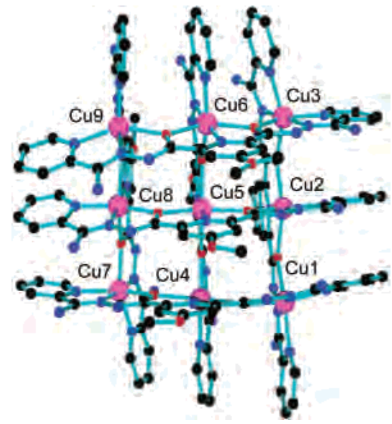


**Figure 6.** Structural representation of the cation in **6** (35% probability thermal ellipsoids).

**[Cu$_9$(m2poap-H)$_2$(m2poap-2H)$_4$](NO$_3$)$_8$·17H$_2$O (6).** Significant disorder problems were encountered during the refinement of the structure of **6**, and there were difficulties identifying all of the expected nitrate anions. However, the grid structure is clearly revealed. Two methoxy groups were found to be disordered on pyridine rings bound to Cu(2) and Cu(6) but were modeled successfully with two methyl positions (C(71) 70%, C(122) 30%; C(51) 60%, C(121) 40%). However, because of disorder problems and a less than ideal refinement ($R_1$ = 0.098, w$R_2$ = 0.346), full details of the structure are not reported at this time. The overall structure is typical of the nonanuclear grids with a [$Cu_9$($\mu$-O)$_{12}$] core and distorted six-coordinate Cu(II) ions. The structure of the cation is shown in Figure 6. Cu−Cu separations fall in the range 3.97−4.21 Å, and Cu−O−Cu angles in the range 135.4−142.4°, with the larger angles involving the central copper Cu(5) (140.3−142.4°). The six-coordinate copper(II) centers have metal−ligand distances in the range 1.90−2.28 Å, with axially elongated geometries ($d_{x^2-y^2}$ ground state) in all cases except Cu(5). The central copper ion has an axially compressed tetragonal structure ($d_{z^2}$ ground state), with long but unequal equatorial contacts (2.18−2.21 Å). As with all $Cu^{II}_9$ complexes of this type, the equatorial (magnetic) planes of the copper ions in the outer ring are not connected directly and are offset, leading to orthogonality between the magnetic orbitals (vide infra). Cu(5) is also considered to be orthogonally arranged because of its nominal $d_{z^2}$ ground state.

**[Cu$_9$(2poap-H)$_4$(picd-H)$_3$(picd-2H)](NO$_3$)$_9$·9H$_2$O (7).** The structure of the cation in **7** is shown in Figure 7, and important bond distances and angles are listed in Table 5. The core structure is shown in Figure 8. Surprisingly the grid contains eight ligands, four 2poap ligands and four pyridine-2,6-dicarboxylates, in a heteroleptic structural arrangement, in keeping with the ratio in which they were

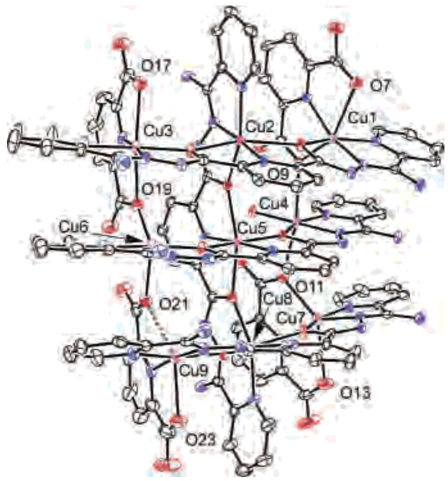


**Figure 7.** Structural representation of the cation in **7** (40% probability thermal ellipsoids).

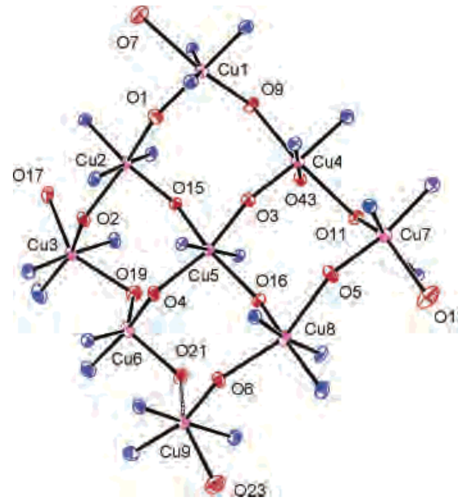


**Figure 8.** Core structure in **7**.

**Table 5.** Selected Bond Distances (Å) and Angles (deg) for **7**

| | | | |
|---|---|---|---|
| Cu(1)−N(28) | 2.019(6) | Cu(5)−O(4) | 2.181(5) |
| Cu(1)−N(1) | 2.050(6) | Cu(5)−O(15) | 2.204(5) |
| Cu(1)−O(9) | 2.215(5) | Cu(5)−O(16) | 2.248(4) |
| Cu(2)−N(32) | 1.912(5) | Cu(6)−N(16) | 1.892(6) |
| Cu(2)−N(5) | 2.008(5) | Cu(6)−O(19) | 1.952(5) |
| Cu(2)−O(15) | 2.022(4) | Cu(6)−O(4) | 1.975(5) |
| Cu(2)−N(30) | 2.064(6) | Cu(6)−N(18) | 1.998(7) |
| Cu(2)−O(2) | 2.312(5) | Cu(6)−O(21) | 2.258(5) |
| Cu(2)−O(1) | 2.354(5) | Cu(7)−N(21) | 1.898(6) |
| Cu(3)−N(7) | 1.899(6) | Cu(7)−N(29) | 2.026(6) |
| Cu(3)−N(39) | 2.029(6) | Cu(7)−O(5) | 2.034(5) |
| Cu(3)−O(2) | 2.030(5) | Cu(7)−N(19) | 2.052(7) |
| Cu(3)−N(9) | 2.063(7) | Cu(7)−O(11) | 2.180(5) |
| Cu(3)−O(17) | 2.386(6) | Cu(8)−N(36) | 1.905(5) |
| Cu(4)−N(12) | 1.910(5) | Cu(8)−N(23) | 2.023(6) |
| Cu(4)−O(43) | 1.937(4) | Cu(8)−O(16) | 2.038(5) |
| Cu(4)−O(3) | 2.021(5) | Cu(8)−N(38) | 2.073(6) |
| Cu(4)−N(10) | 2.049(6) | Cu(8)−O(6) | 2.309(5) |
| Cu(4)−O(9) | 2.429(5) | Cu(9)−N(25) | 1.897(6) |
| Cu(5)−N(14) | 1.920(5) | Cu(9)−O(6) | 1.992(5) |
| Cu(5)−N(34) | 1.938(5) | Cu(9)−N(27) | 2.016(6) |
| Cu(5)−O(3) | 2.101(5) | Cu(9)−N(40) | 2.018(6) |
| Cu−Cu (ring) | 3.678−4.275 | Cu−Cu (center) | 3.861−4.055 |
| Cu(1)−O(1)−Cu(2) | 141.0(2) | Cu(3)−O(19)−Cu(6) | 112.2(2) |
| Cu(3)−O(2)−Cu(2) | 141.5(2) | Cu(6)−O(21)−Cu(9) | 118.5(2) |
| Cu(4)−O(3)−Cu(5) | 139.0(2) | Cu(7)−O(5)−Cu(8) | 142.3(2) |
| Cu(6)−O(4)−Cu(5) | 139.5(2) | Cu(4)−O(11)−Cu(7) | 118.8(2) |
| Cu(9)−O(6)−Cu(8) | 142.0(2) | Cu(2)−O(15)−Cu(5) | 139.9(2) |
| Cu(1)−O(9)−Cu(4) | 121.7(2) | Cu(5)−O(16)−Cu(8) | 142.2(2) |

reacted (vide ante). All the ligands encapsulate the nonacopper core, which has the familiar [$Cu_9(\mu\text{-}O)_{12}$] grid arrangement observed in e.g. **5** and **6** and other examples. Three 2poap ligands bind to one face of the grid, with alkoxide oxygen atoms bridging the metal ions. On the other face one 2poap ligand occupies the central ligand site, but four independent pyridine-2,6-dicarboxylate (picd) ligands position themselves above the corner copper centers, in a tridentate fashion, but remarkably the inner donor oxygen atoms (O(9), O(11), O(19), O(21)) actually bridge the adjacent copper atoms, thus effectively completing the ($\mu$-O)$_{12}$ core arrangement. However, the core (Figure 8) is highly distorted in comparison with the homoleptic systems. All the copper(II) ions can be considered to be pseudooctahedral, with varying degrees of distortion, except for Cu(6), which is five-coordinate. Cu(4) completes its six coordination with a short bond to what is assumed to be a water molecule (O(43); 1.937(4) Å). The central copper, Cu(5), has a tetragonally compressed ($d_{z^2}$) structure, typical of the homoleptic grids, with four long connections to adjacent oxygen atoms and short axial connections to the central pyridine nitrogen atoms. The corner copper ions have *mer*-$N_3O_3$ donor groupings, compared with *cis*-$N_4O_2$ for the homoleptic systems. The side copper atoms Cu(2) and Cu(8) have *mer*-$N_3O_3$ structures, while Cu(4) is *cis*-$N_2O_4$ and Cu(6) has a distorted square-pyramidal $N_2O_3$ structure.

Cu−Cu separations in the outer $Cu_8$ ring fall in the range 3.678−4.275 Å and in the inner segment in the range 3.861−4.055 Å. The very short Cu(3)−Cu(6) distance (3.678(4) Å) signals a very small Cu−O−Cu angle (112.2(2)°), which is characteristic of the carboxylate oxygen bridging connections in general (Cu−O−Cu 112−122°). The other Cu−O(alkoxide)−Cu angles fall in the range 139−143°, typical of the homoleptic systems in this class. Defining the magnetic ground states of the copper ions is very important in terms of mapping out the "magnetic connections" between the copper centers. The corner copper ions Cu(1), Cu(3), Cu(7), and Cu(9) have tetragonally elongated $d_{x^2-y^2}$ ground states, with long bonds to O(9), O(19), O(11), and O(21), respectively. Cu(2), Cu(4), and Cu(8) also have tetragonally elongated $d_{x^2-y^2}$ ground states each with two long contacts to O(1) and O(2), O(9) and O(11), and O(5) and O(6), respectively. Cu(6) has a $d_{x^2-y^2}$ ground state also with a long connection to O(21). Cu(5) has a $d_{z^2}$ ground state and long equatorial connections to its neighboring oxygen donors. This overall connectivity gives the whole molecule nominal total magnetic orbital "orthogonality" (vide supra).

The most remarkable feature of the structure rests with the presence of two such different ligands in the same molecule. This has been observed once before with the complex [$Cu_9$(m2poap-2H)$_4$(Clpic)$_2$]($NO_3$)$_6$·22$H_2O$[14] (Clpic = 4-chloro-2,6-dipicolinate), but in this case the picolinate residues occupied bridging positions on two end copper triads. A reasonable argument for self-assembly of these nonanuclear grids lies with the encoded coordination site information within each ligand pocket and the effective way in which their aromatic rings adopt a parallel arrangement with separations approaching van der Waals contacts, clearly indicating the importance of $\pi$ interactions between the ligands. The structure of **7** clearly illustrates the fact that six fully tritopic ligands are not necessary and the grid outcome can effectively be defined by just four. That the pyridine dicarboxylate ligands add on to the corner copper atoms in this case is clearly associated with their similar "bite" to the ends of 2poap, but the bridging nature of the carboxylate oxygen atoms is quite remarkable. Ligand–ligand contacts are quite short (3.6 Å and above), and despite the fact that the picolinate ligand pyridine rings are offset slightly relative the terminal pyridine rings of the central 2poap, inter-ring contacts are still considered to be a stabilizing influence in grid formation.

**Solvent and Temperature-Dependent Oligomer Formation and Interconversion.** The formation of **1** occurs at room temperature in high yield in acetonitrile/methanol mixture, while in a more polar aqueous solvent mixture and with warming the $Cu_9$ complex **5** forms in high yield. Given the nonhomoleptic nature of **1**, and the fact that the external copper centers adopt a preferred five-coordinate copper(II) geometry, it is reasonable to assume that the weakly coordinating solvent mixture allows the nitrate ions to act as ligands and achieve a "stable" $Cu_8$ oligomeric form. In the case of the previously reported $Cu_8$ pinwheel structure[18] involving 2poap, the Gd(III) ions may have played a minor role in the structural outcome, but the dominant effects appear to be the nature of the solvent and the temperature. The presence of a more polar solvent mixture (methanol/water as opposed to acetonitrile/methanol) would make the nitrate coordination less likely and with increased temperature leads to the formation of the more thermodynamically favored homoleptic $Cu_9$ grid complex. As a test of the increased stability of **5** compared with **1**, a sample of **1** was dissolved in a methanol/water mixture and the solution warmed. On standing red-orange crystals are formed, which have been shown to be the $Cu_9$ grid complex **5** (identical infrared spectrum and magnetic properties and consistent elemental analysis).

Complex **2** is derived from a different Schiff base ligand and appears to preferentially form the $Cu_8$ pinwheel cluster, with no indication that it can be converted to the $Cu_9$ grid, despite several attempts. Complex **6** also appears to be the only product formed in the reaction between m2poap and $Cu(NO_3)_2 \cdot 3H_2O$, even with varying reaction conditions and solvent. The unprecedented pinwheel $Cu_8$ cluster structure observed for **4**, with mixed bridging ligand groups, clearly highlights the versatility of ligands in this class, and 2pomp joins e.g. poap in this regard.[25]

**Magnetic Properties.** The completely different structures of **1**–**4** ($Cu_8$ pinwheels) and **5**–**7** ($Cu_9$ [3 × 3] grids) leads to magnetic exchange models, which are of necessity very different, and magnetic properties that would be expected to be quite different. However both types of compound are dominated by intramolecular ferromagnetic coupling. Figure 9 shows the magnetic models for the two cases, both of which include two different $J$ values. The corresponding exchange Hamiltonian expressions for these models are given

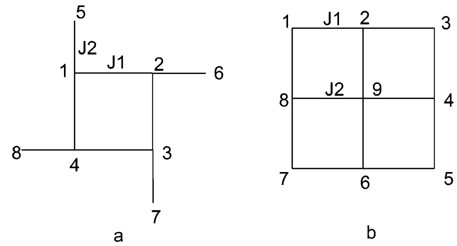


**Figure 9.** Magnetic exchange models for **1**–**7**.

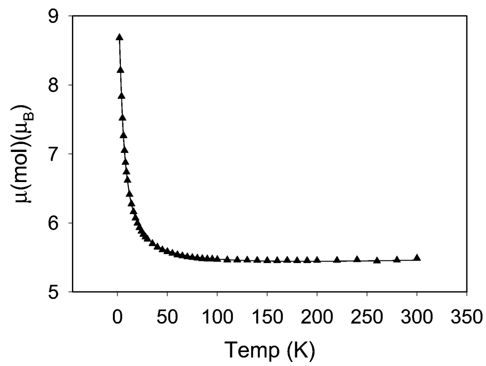


**Figure 10.** Plot of magnetic moment/mol as a function of temperature for **1**. The solid line represents the best fit to eqs 1 and 3, with $g = 2.15(1)$, $J = 7.8(5)$ cm$^{-1}$, TIP = 540 × 10$^{-6}$ emu·mol$^{-1}$, and $\Theta = -0.10$ K ($10^2R = 0.47$).

in eqs 1 and 2. The total spin state ($S'$) values, and their energies, for all spin vector combinations were evaluated, using normal vector addition principles,[27]

$$H_{ex} = -J_1\{S_1S_2 + S_2S_3 + S_3S_4 + S_1S_4\} - J_2\{S_1S_5 + S_2S_6 + S_3S_7 + S_4S_8\} \quad (1)$$

$$H_{ex} = -J_1\{S_1S_2 + S_2S_3 + S_3S_4 + S_4S_5 + S_5S_6 + S_6S_7 + S_7S_8 + S_1S_8\} - J_2\{S_2S_9 + S_4S_9 + S_6S_9 + S_8S_9\} \quad (2)$$

$$\chi_M = \frac{N\beta^2 g^2}{3k(T-\Theta)} \frac{\Sigma S'(S'+1)(2S'+1)e^{-E(S')/kT}}{\Sigma(2S'+1)e^{-E(S')/kT}} + \mathrm{TIP} \quad (3)$$

and substituted into the Van Vleck equation (eq 3) within the internal structure of the software package MAGMUN4.0,[28] to calculate the temperature variation of molar susceptibility ($\chi_M$). A Weiss-like temperature correction ($\Theta$) to account for intermolecular exchange effects and a correction for temperature-independent paramagnetism (TIP) are applied. The variable-temperature magnetic data ($\mu_{mol}$) for **1** are shown in Figure 10. The room-temperature moment value (5.5 $\mu_B$/mol) is well above the spin-only value for eight Cu(II) centers (4.9 $\mu_B$) and rises as temperature is lowered to 8.7 $\mu_B$ indicative of significant ferromagnetic exchange within the cluster. The magnetic data were fitted to eqs 1 and 3 within MAGMUN4.0, but the calculation was simpli-

(27) Kambe, K. *J. Phys. Soc. Jpn.* **1950**, *5*, 48.
(28) MAGMUN4.0 is available free of charge from http://www.ucs.mun.ca/~lthomp/index.html. It has been developed by Dr. Zhiqiang Xu (Memorial University), in conjunction with Dr. O. Waldmann (waldmann@mps.ohio-state.edu). We do not distribute the source codes. The programs may be used only for scientific purposes, and economic utilization is not allowed. If the routine is used to obtain scientific results, which are published, the origin of the programs should be quoted.

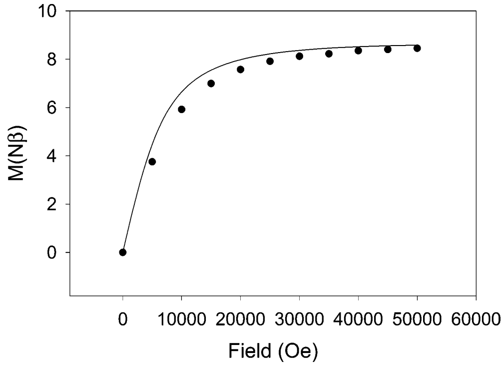


**Figure 11.** Magnetization data for **1** as a function of field at 2 K. The solid line is calculated for $g = 2.15$ and $S = 8/2$.

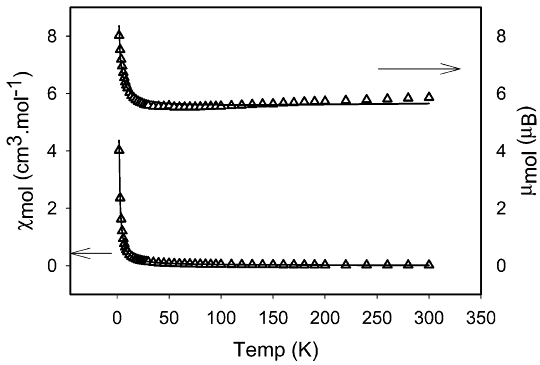


**Figure 12.** Variable-temperature magnetic data for **4**. The solid lines represent the best fit to eqs 1and 3 with $g = 2.24(3)$, $J_1 = 6.1(9)$ cm$^{-1}$, $J_2 = -1.5(5)$ cm$^{-1}$, TIP = 700 $\times$ 10$^{-6}$ cm$^3$·mol$^{-1}$, and $\Theta = 1.2$ K ($10^2R$ = 4.6).

fied by assuming that $J = J_1 = J_2$, because of the similarity of the bridging groups throughout the molecule. The best data fit gave $g = 2.15(1)$, $J = 7.8(5)$ cm$^{-1}$, TIP = 540 $\times$ 10$^{-6}$ emu·mol$^{-1}$, $\Theta = -0.10$ K ($10^2R = 0.47$; $R = [\Sigma(\chi_{obsd} - \chi_{calcd})^2/\Sigma\chi_{obs}{}^2]^{1/2}$). The solid line in Figure 10 was calculated with these parameters. The $J$ value is consistent with the related $Cu_8$ pinwheel cluster ($[Cu_8(2poap)_4(CH_3OH)_4(CH_3CN)_4][Gd(NO_3)_4(H_2O)_2]_2(NO_3)_6 \cdot 1.3Cu(NO_3)_2 \cdot 10H_2O$)[18] but should be considered a more accurate evaluation of the exchange within the cluster itself, since the mononuclear and highly paramagnetic Gd(III) centers, which are present in the former case and dominate the overall magnetic properties, do not exist in **1**. Magnetization data were collected as a function of field at 2 K (Figure 11) and show that the system is almost saturated at high field. The solid line is calculated using the appropriate Brillouin function for $S = 8/2$ and $g = 2.15$ (the same "$g$" value as obtained above) at 2 K and is very close to the experimental data. The slightly depressed profile compared with the theoretical line suggests a minor antiferromagnetic component, which is likely to be intermolecular in nature, as suggested by the small negative $\Theta$ value. The ferromagnetic exchange in **1** is expected on the basis of the strictly orthogonal arrangement of the copper magnetic orbitals throughout the structure.

Compounds **2** and **3** exhibit similar profiles of magnetic moment as a function of temperature, with moment rising smoothly as temperature is lowered. Fitting of the variable-temperature data to eqs 1 and 3 ($J = J_1 = J_2$) gave $g = 2.18(2)$, $J = 4.9(4)$ cm$^{-1}$, TIP = 410 $\times$ 10$^{-6}$ emu·mol$^{-1}$, $\Theta = -1.0$ K ($10^2R = 1.34$) for **2** and $g = 2.13(3)$, $J = 4.3(6)$ cm$^{-1}$, TIP = 500 $\times$ 10$^{-6}$ emu·mol$^{-1}$, and $\Theta = 0.2$ K ($10^2R = 2.4$) for **3**. These results are reasonable on the basis of the similarity of the structures of **1** and **2** and indicate clearly that **3** has a similar pinwheel structure. The slight difference in the magnetic properties of **2** and **3** compared with **1** may be associated with the slight differences in the ligand (e.g. $CH_3$ versus $NH_2$), leading to differences in the metal ion coordination spheres. Magnetization profiles as a function of field for **2** and **3** at 2 K are similar to that observed for **1**, indicating $S = 8/2$ ground states.

Compound **4** is an unusual case, with two different bridges, but the structure suggests that antiferromagnetic exchange terms are unlikely to be important, because of the nominally orthogonal connections through the N−N bridges. The plots of the temperature variation of magnetic susceptibility and magnetic moment are illustrated in Figure 12. The magnetic moment drops slightly from 5.85 $\mu_B$ at 300 K to 5.52 $\mu_B$ at 65 K, followed by a steep rise to 8.02 $\mu_B$ at 2 K. The overall shape is typical of the ferromagnetic pinwheel clusters, but the slight downward trend in moment is unusual and suggests that a weak antiferromagnetic effect is present as well. Fitting the data to eqs 1 and 3 gave $g = 2.24(3)$, $J_1 = 6.1(9)$ cm$^{-1}$, $J_2 = -1.5(5)$ cm$^{-1}$, TIP = 700 $\times$ 10$^{-6}$ cm$^3$·mol$^{-1}$, and $\Theta = 1.2$ K ($10^2R = 4.6$). The solid lines in Figure 12 are calculated with these parameters. The requirement of a negative $J_2$ is surprising but confirms the expected antiferromagnetic term, which is associated with the diazine N−N bridging connections. Field-dependent magnetization data at 2 K show that **4** approaches saturation at 5 T ($M = 7.9$ $N\beta$) but with values close to those calculated for an $S = 7/2$ rather than an $S = 8/2$ ground-state species. This is in agreement with the presence of a weak antiferromagnetic component. An examination of the structure of **4** shows that the direct Cu(2)−N(3)−N(2)−Cu(1) bridge should be orthogonal (Cu(2)−N(3) 2.443 Å), despite the large C−N−N−Cu torsional angle (such large Cu−N−N−Cu angles have been shown to lead to quite strong antiferromagnetic exchange when copper magnetic orbitals are connected directly[29,30]), and so any antiferromagnetic term would be expected to be very small and probably insignificant. However, an alternate five bond equatorial and nonorthogonal, "magnetic connection" exists through the ligand backbone itself (Cu(2)−O(1)−C(8)−C(9)−N(4)−Cu(1)), which could provide the weak antiferromagnetic exchange pathway.

Figure 13 shows the profile of magnetic moment/mol for **5** as a function of temperature, with a room-temperature value of 5.8 $\mu_B$, dropping to 5.4 $\mu_B$ at 20 K, followed by a rise 6.5 $\mu_B$ at 2 K. This is typical of the magnetic behavior of the $Cu_9$ square [3 $\times$ 3] grids as a whole,[10,11] and the profile is symbolic of a combination of both intramolecular antiferromagnetic and ferromagnetic coupling, with the antiferromagnetic component dominating at temperatures >20 K. The preliminary structure clearly reveals the $Cu_9$ grid arrange-

(29) Xu, Z.; Thompson, L. K.; Miller, D. O. *Inorg. Chem.* **1997**, *36*, 3985.
(30) Thompson, L. K.; Xu, Z.; Goeta, A. E.; Howard, J. A. K.; Clase, H. J.; Miller, D. O. *Inorg. Chem.* **1998**, *37*, 3217.

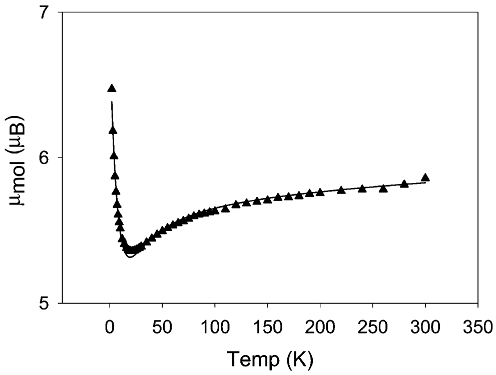


**Figure 13.** Plot of magnetic moment/mol as a function of temperature for **5**. The solid line represents the best fit to eqs 2 and 3 with $g = 2.29(5)$, $J_1 = 0.87(4)$ cm$^{-1}$, $J_2 = -17.9(7)$ cm$^{-1}$, TIP $= 550 \times 10^{-6}$ emu·mol$^{-1}$, and $\Theta = -0.3$ K ($10^2R = 0.91$).

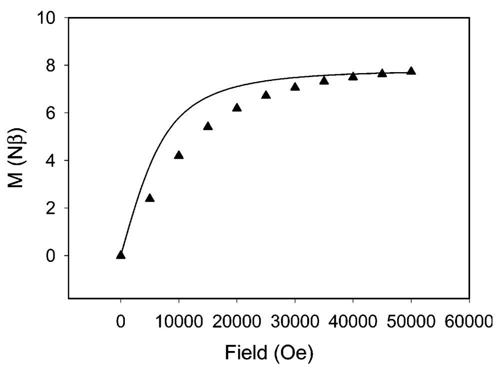


**Figure 14.** Magnetization data for **5** as a function of field at 2 K. The solid line is calculated for $g = 2.29$ and $S = 7/2$.

ment, and this is confirmed by the magnetic data. The magnetic data were fitted successfully to eqs 2 and 3, with $g = 2.29(5)$, $J_1 = 0.87(4)$ cm$^{-1}$, $J_2 = -17.9(7)$ cm$^{-1}$, TIP $= 550 \times 10^{-6}$ emu·mol$^{-1}$, and $\Theta = -0.30$ K ($10^2R = 0.91$). The solid line in Figure 13 was calculated with these parameters. Magnetization data at 2 K, as a function of field, show that **5** is almost saturated at 5.0 T, with an $N\beta$ value consistent with an $S = 7/2$ ground state. Figure 14 compares the experimental values with calculated values for $g = 2.29$ and $S = 7/2$ at 2 K. The slightly lower experimental profile may be associated with an intermolecular antiferromagnetic association, as suggested by the small negative $\Theta$ value. It is interesting to note that while $J_1$ is comparable to $J_1$ for the analogous grid complex $[Cu_9(2poap)_6](NO_3)_{12}\cdot 9H_2O$ ($J_1 = 0.52$ cm$^{-1}$, $J_2 = -24.3$ cm$^{-1}$),[10,11,13] $|J_2|$ is somewhat smaller. This could be rationalized in terms of the presence of electron-withdrawing chlorine atoms on the two central pyridine rings, which are bonded to the central copper.

**6** exhibits similar magnetic properties, expected on the basis of the grid structure (Figure 6), with magnetic moment dropping from 5.84 $\mu_B$ (per mole) at 300 K to a minimum value of 5.16 $\mu_B$ at 26 K, followed by a sharp rise to 6.39 $\mu_B$ at 2 K. The magnetic data were fitted successfully to eqs 2 and 3 giving $g = 2.17(1)$, $J_1 = 0.5(1)$ cm$^{-1}$, $J_2 = -23(1)$ cm$^{-1}$, TIP $= 790 \times 10^{-6}$ emu·mol$^{-1}$, and $\Theta = 0$ K ($10^2R = 1.85$). $J_1$ and $J_2$ are comparable with the values observed for $[Cu_9(2poap)_6](NO_3)_{12}\cdot 9H_2O$.[10,11,13] Magnetization data as a function of field at 2 K show a typical profile with M rising steeply and approaching saturation at 5.0 T with $M = 7.1$ $N\beta$.

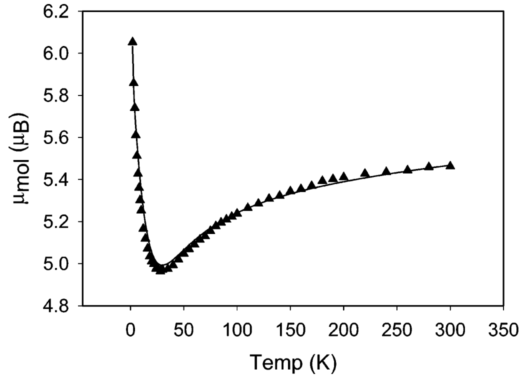


**Figure 15.** Plot of magnetic moment/mol as a function of temperature for **7**. The solid line represents the best fit to eqs 2 and 3 with $g = 2.09(1)$, $J_1 = 0.5(2)$ cm$^{-1}$, $J_2 = -29(2)$ cm$^{-1}$, TIP $= 550 \times 10^{-6}$ emu.mol$^{-1}$, and $\Theta = 0$ K ($10^2R = 1.3$).

The positive ferromagnetic $J_1$ observed for both **5** and **6** is directly associated with the orthogonal bridging arrangement between the eight copper atoms in the outer ring, while the negative, antiferromagnetic $J_2$ is unusual but typical of these systems and has been rationalized in terms of a fluxional magnetic ground state associated with the unusual, tetragonally compressed ($d_{z^2}$ ground state) central copper. On the basis of the $d_{z^2}$ ground state one would nominally expect not to have antiferromagnetic exchange involving the central copper, but the clearly defined $J_2$ indicates that on average this metal center interacts with one adjacent copper antiferromagnetically. This is indicative of a possible dynamic Jahn−Teller distortion at the central copper, or a mixed orbital ground-state situation.

The variable-temperature magnetic data for **7** are very similar to those of **5** and **6**, with magnetic moment dropping from 5.5 $\mu_B$ at 300 K to 4.9 $\mu_B$ at ~30 K, followed by a sharp rise at lower temperatures to 6.1 $\mu_B$ at 2 K (Figure 15), behavior typical of a grid exhibiting both ferromagnetic and antiferromagnetic exchange. The data were fitted successfully to eqs 2 and 3 for $g = 2.09(1)$, $J_1 = 0.5(2)$ cm$^{-1}$, $J_2 = -29(2)$ cm$^{-1}$, TIP $= 550 \times 10^{-6}$ emu·mol$^{-1}$, and $\Theta = 0$ K ($10^2R = 1.3$). The solid line in Figure 15 is calculated with these parameters. Magnetization data as a function of field at 2 K indicate that the system is not fully saturated at 5.0 T (50 000 Oe) but approaches the expected $S = 7/2$ ground state. This is probably associated with the quite distorted and more flexible nature of the grid core and the larger than usual antiferromagnetic $J_2$ term. However, what is remarkable is the fact that the magnetic properties of **7** are typical of the usual homoleptic $[Cu_9(\mu\text{-}O)_{12}]$ grids, despite the fact that four oxygen bridges are from carboxylate oxygen atoms and not alkoxide oxygens and that the complex contains a mixture of ligands.

## Conclusion

It has been demonstrated that two oligomers can be produced with the ligand Cl2poap in self-assembly reactions with copper nitrate, depending on solvent and temperature, and that the alkoxide bridged pinwheel $Cu_8$ cluster can be converted to the more thermodynamically favored, alkoxide-bridged $Cu_9$ [3 × 3] grid. In the case of Cl2pomp conversion of the pinwheel cluster to the $Cu_9$ [3 × 3] grid form does not appear to occur, at least under the conditions tested. On the other hand m2poap forms a $Cu_9$ [3 × 3] with no tendency to form a $Cu_8$ structure. Another pinwheel $Cu_8$ cluster is observed with the ligand 2pomp, in which there are two different bridging groups, $\mu_2$-(N−N) and $\mu_2$-alkoxide, indicating again the coordinative flexibility of this class of ligands. With a mixture of 2poap and pyridine-2,6-dicarboxylic acid a remarkable $[Cu_9(\mu\text{-}O)_{12}]$ [3 × 3] grid results, with four pyridine dicarboxylate ligands effectively occupying the normal position of two 2poap ligands. This indicates that grid construction can be accomplished with different ligand mixtures, perhaps opening up a way to grids of different and varied dimensions. Magnetic properties are interpreted in terms of dominant ferromagnetic coupling within both types of self-assembled supramolecular system, which shows up clearly at low temperatures, and is associated with orthogonal bridging arrangements. The magnetic ground state for **1**−**3** ($S = 8/2$) indicates that all interactions are ferromagnetic, but for **4** there is evidence for a weak intramolecular antiferromagnetic component. For **5**−**7** a putative fluxional magnetic ground state at the central copper leads to an overall $S = 7/2$ spin ground state for the grids, resulting from the compensating effects of ferromagnetic and antiferromagnetic exchange components.

**Acknowledgment.** We thank the NSERC (Natural Sciences and Engineering Research Council of Canada) and the Research Council of Norway (H.G.) for financial support and Dr. R. McDonald, University of Alberta, for structural data.

**Supporting Information Available:** X-ray crystallographic data in CIF format for **1**, **2**, **4**, and **7**. This material is available free of charge via the Internet at http://pubs.acs.org. Crystallographic data for **1**, **2**, **4**, and **7** have also been deposited with the Cambridge Crystallographic Data Center, CCDC Nos. 206673, 206674, 206676, and 223491. Copies of this information may be obtained free of charge from The Director, CCDC, 12, Union Road, Cambridge CB2 1EZ, U.K. (fax +44-1223-336033; E-mail deposit@ccdc.cam.ac.uk; http://www.ccdc.cam.ac.uk).

IC030113U